Published in final edited form as:
Am J Physiol Renal Physiol. 2008 April ; 294(4): F919–F927. doi:10.1152/ajprenal.00265.2007.

Studies on localization and function of annexin A4a within urinary bladder epithelium using a mouse knockout model

Warren G. Hill[1], **Susan Meyers**[3], **Maximilian von Bodungen**[1], **Gerard Apodaca**[3], **John R. Dedman**[4], **Marcia A. Kaetzel**[4], and **Mark L. Zeidel**[2]

[1]Division of Matrix Biology, Harvard Medical School, Beth Israel Deaconess Medical Center, Boston, Massachusetts

[2]Department of Medicine, Harvard Medical School, Beth Israel Deaconess Medical Center, Boston, Massachusetts

[3]Renal-Electrolyte Division, Department of Medicine, University of Pittsburgh School of Medicine, Pittsburgh, Pennsylvania

[4]Department of Molecular Oncogenesis, University of Cincinnati Genome Research Institute, Cincinnati, Ohio

Abstract

Annexin A4 (anxA4) is a member of the Ca^{2+}-dependent membrane-binding family of proteins implicated in the regulation of ion conductances, Ca^{2+} homeostasis, and membrane trafficking. We demonstrate, in mice, that annexins 1-6 are present in whole bladder and exhibit differential expression in the urothelium. An anxA4a-knockout ($anxA4a^{-/-}$) mouse model shows no protein in the urothelium by immunofluorescence and immunoblotting. In wild-type bladders, anxA4a in umbrella cells showed uniform cytoplasmic staining and some association with the nuclear membrane. Application of a hydrostatic pressure to bladders mounted in Ussing chambers resulted in redistribution of anxA4a from cytoplasm to cellular boundaries in the basal and intermediate cells but not in superficial umbrella cells. We hypothesized that anxA4a might be important for barrier function or for stretch-activated membrane trafficking. To test these hypotheses, we conducted a series of functional and morphological analyses on bladders from control and $anxA4a^{-/-}$ animals. The transepithelial resistances, water permeabilities, and urea permeabilities of $anxA4a^{-/-}$ bladders were not different from controls, indicating that barrier function was intact. Membrane trafficking in response to hydrostatic pressure as measured by capacitance increases was also normal for $anxA4a^{-/-}$ bladders. Cystometrograms performed on live animals showed that voiding frequency and intrabladder pressures were also not different. There were no differences in bladder surface morphology or cellular architecture examined by scanning and transmission electron microscopy, respectively. We conclude that loss of anxA4 from the urothelium does not affect barrier function, membrane trafficking, or normal bladder-voiding behavior.

Keywords

permeability; barrier; trafficking

Address for reprint requests and other correspondence: M. L. Zeidel, Beth Israel Deaconess Medical Center, 330 Brookline Ave., YA419, Boston, MA 02215 (e-mail: mzeidel@bidmc.harvard.edu)..

ANNEXINS ARE A UBIQUITOUS protein family characterized by an ability to bind to phospholipids at membrane surfaces in response to elevated Ca^{2+}. Two structural motifs occur in all members: *1*) a highly conserved phospholipid-binding domain consisting of four repeat stretches of 70 amino acids packed into an α-helical disk and *2*) the NH_2 terminus, which varies in length and sequence between family members and appears to differentiate the cellular function and location. Although the phospholipid-binding activity has been characterized structurally, chemically, and kinetically (2,13,20,22,23,26,27,29), the physiological role of these proteins is not well understood. Broad themes in terms of cellular function have been uncovered, but the precise role of these proteins is unclear (for review see Ref. 10). Because of the ability of annexins to bind to and "annex" or aggregate membrane surfaces, they appear to participate in Ca^{2+}-regulated membrane dynamics. Thus they have been shown to be involved in exocytosis (10), membrane domain organization (9,17), and ion channel activity regulation (14).

Annexin A4 (anxA4), the subject of this study, is found at high levels in secretory epithelia in the lung, intestine, stomach, and kidney. Gene trap disruption of the first intron revealed that there were in fact three splice variants of anxA4 with differing tissue expression (21). The knockout animal lacked the major transcript, anxA4a, which has a broad tissue distribution. However, two further transcripts, designated anxA4b and anxA4c, were unaffected by the intron disruption in this region. anxA4b was shown to be expressed only in the digestive tract and anxA4c exhibited a restricted expression pattern within solitary chemosensory cells. In nonstratified epithelia, they extend from the basement membrane to the lumen and appear to perform paracrine/endocrine functions (21). We now demonstrate for the first time that the major transcript of anxA4, anxA4a, is present in the superficial and transitional epithelium of the bladder, where it is expressed throughout the urothelium. Umbrella cells have large numbers of unique elongated vesicles underlying the apical membrane. These "fusiform vesicles" are thought to play a key role in the bladder's ability to stretch by providing a large amount of membrane available for exocytosis and endocytosis. This allows umbrella cells to increase their apical surface area in response to filling and then to decrease it upon emptying.

Since urine has osmolalities that can vary from 50 to 1,000 mosmol/kg in humans and from 2,000 to 4,000 mosmol/kg in the mouse (16), widely fluctuating urea and NH_3 concentrations, and proton concentrations that vary over many orders of magnitude (pH 4.5-9), the bladder permeability barrier plays an essential role in osmotic and metabolic homeostasis. It has been shown that anxA4 binding and self-polymerization on membranes results in a rigidification of the lipids in the bound leaflet, with a resulting reduction in the permeability of the membrane to water and protons (11). Cells could, in theory, acutely regulate their membrane permeability through Ca^{2+} signaling pathways that initiate anxA4 binding to the inner surface of the plasma membrane. Such activity in the bladder might represent an important mechanism for regulating epithelial barrier function. Given the biophysical properties and urothelial expression of anxA4, we hypothesized that this annexin could be important to the integrity or the regulation of the bladder permeability barrier.

Bladder filling has been shown to activate a complex set of mechanosensitive responses in umbrella cells, including ATP release and purinergic receptor-dependent membrane trafficking (32). Hydrostatically induced stretch has been shown to raise intracellular Ca^{2+} in the urothelium; furthermore, blocking Ca^{2+} release from intracellular stores inhibited exocytosis (32). Given the known membrane-organizing ability of annexins and sensitivity to Ca^{2+}, we also investigated the hypothesis that anxA4 might play a specific role in umbrella cell membrane trafficking.

We demonstrate in wild-type bladders that stretch induces a redistribution of anxA4 within basal and intermediate cells to the cellular periphery. To explore several possible physiological roles for anxA4a in mammalian bladder, we utilized a genetically modified mouse model in which the protein is not expressed in renal epithelia (21). Comparison with wild-type animals revealed no alterations in normal bladder function or morphology in the anxA4a$^{-/-}$ animals, suggesting that the role of anxA4 in the bladder does not include barrier function or stretch-regulated intracellular trafficking.

METHODS

Mouse strains

Generation of anxA4a gene-disrupted mice was accomplished by a retrovirus-mediated gene trap strategy that randomly integrates a construct into genomic DNA (21). The gene trap was determined to be inserted into the first intron of the anxA4 gene at nucleotide 24790, 3′ downstream of exon a (10001) and 5′ upstream of exon 1 (37788). These mice have been fully characterized elsewhere (21), and genetic analysis revealed the presence of two alternatively spliced transcripts. Each of the three transcripts produces the same 35-kDa protein, so tissues that express either of the other two minor anxA4 transcripts are positive for the presence of anxA4 protein. In anxA4a$^{-/-}$ mice, anxA4 protein was absent from most tissues, but it was still present in intestine.

Immunohistochemistry

Bladders from wild-type and anxA4a$^{-/-}$ mice were removed, fixed in 10% formalin, embedded in paraffin, and cut into 4-μm-thick sections. Deparaffinized sections were blocked with 10% rabbit serum and incubated with affinity-purified sheep anti-anxA4 and then with FITC-rabbit anti-sheep secondary antibody (15). Fluorescent images were observed on a Nikon Eclipse E600W microscope using a ×40 objective and digitally recorded using a Nikon Coolpix E8700 camera.

Immunoblot analysis

Bladders were harvested, immediately frozen on dry ice, crushed, homogenized in sample buffer, subjected to 12% SDS-PAGE, and transferred to a polyvinylidene difluoride membrane. Four bladders were pooled for each genotype. For detection of annexins 1-6, membranes were incubated in monospecific affinity-purified primary antibodies prepared as described elsewhere (15) and then in peroxidase-labeled secondary antibodies and exposed to ECL chemiluminescent substrate, and the film was exposed according to the manufacturer's instructions (GE Amersham).

Immunofluorescent labeling of cryosectioned bladders and confocal laser scanning microscopy

Mice were euthanized by inhalation of 100% CO_2. Their bladders were excised, placed in Krebs buffer [in mM: 110 NaCl, 5.8 KCl, 25 $NaHCO_3$, 1.2 KH_2PO_4, 2.0 $CaCl_2$, 1.2 $MgSO_4$, and 11.1 glucose (pH 7.4) at 37°C, bubbled with 95% O_2-5% CO_2 gas], and mounted on rings that exposed 0.28-cm^2 tissue surface area. Dissection of the muscularis on the rings under a stereomicroscope left only the intact urothelium and varying amounts of adjacent connective tissue. The tissue was mounted in Ussing chambers as described previously (31) and allowed to equilibrate for 60 min. Bladder filling was mimicked by filling the mucosal chamber, creating a backpressure of ~1 cmH_2O for 60 min. While in the chamber, bladders were fixed using 4% paraformaldehyde as described previously (1). A cryostat (model HM 505N, Micron International) was used to cut 4-μm-thick sections, which were prepared for immunofluorescence staining. Staining for anxA4 was performed as described elsewhere (1)

using a sheep polyclonal anti-anxA4 primary antibody (15) at 1:20 dilution for 60 min at room temperature and FITC-conjugated rabbit anti-sheep IgG at 1:100 dilution for 60 min as secondary antibody. Antibodies to annexins (generated in the laboratory of J. R. Dedman) were used at dilutions of 1:2.5 (annexin 2) and 1:100 (annexins 1, 3, 5, and 6). Sections were counterstained for nuclei with TO-PRO-3 iodide (Invitrogen) at 1:100 dilution for 60 min. Confocal microscopy was performed on a confocal microscope (LSM 510 META, Carl Zeiss MicroImaging) using a ×60 objective. Single-focal-plane images were acquired three times and averaged to reduce noise.

Measurement of uroepithelial barrier function

Transepithelial resistance (TER) and urea and water permeability were measured as described elsewhere (12). Briefly, excised bladders mounted in Ussing chambers and bathed in Krebs buffer, stirred, oxygenated, and maintained at 37°C were exposed to tritiated water (1 μCi/ml) and [^{14}C]urea (0.25 μCi/ml) on the apical side. Two 100-μl aliquots were removed from the basolateral and apical chambers for scintillation counting and volume was replaced at 15-min intervals. TER was monitored by use of Ag-AgCl current and voltage electrodes connected to an epithelial voltage clamp (model EC825, Warner). (For further details of the technique and calculations of permeability coefficients see Refs. 18 and 19.)

Electron microscopy

Electron microscopy was performed as described elsewhere (4). Mouse bladders were placed in fixative containing 2.0% (vol/vol) glutaraldehyde and 2.0% (wt/vol) paraformaldehyde in 100 mM sodium cacodylate (pH 7.4), 1 mM $CaCl_2$, and 0.5 mM $MgCl_2$ for 60 min at room temperature.

The fixed tissue was washed for 15 min en bloc in 100 mM sodium cacodylate buffer (pH 7.4) and then treated with 1% (wt/vol) OsO_4 in 100 mM sodium cacodylate buffer (pH 7.4) for 60 min at 4°C. After several water rinses, the samples were stained en bloc overnight with 0.5% uranyl acetate in water. Samples were dehydrated in a graded series of ethanol [40, 50, 75, 80, 90, 95, and 100% (vol/vol) in water] and then in 100% propylene oxide (EMS, Hatfield, PA). Tissues were embedded in epoxy resin (LX-112, Ladd) and sectioned with a diamond knife (Diatome). Sections were mounted on butvar-coated copper grids, contrasted with uranyl acetate and lead citrate, and viewed at 80 kV in an electron microscope (100 CX, Jeol). Images were captured on Kodak electron microscopy film, developed, and then printed with a MohrPro 8 processor. Graphs were scanned, and contrast was corrected in Photoshop CS (Adobe). All images are representative of similar results obtained from the bladders of at least three animals.

Capacitance measurements

A modified Ussing chamber was used to monitor changes in uroepithelial capacitance upon stretch; changes in apical surface area were carefully measured. Mouse bladders were excised and placed in Krebs buffer (pH 7.4 at 37°C, bubbled with 95% O_2-5% CO_2 gas). Each bladder was cut open and then mounted on a Delrin ring that exposed 0.28 cm of tissue. The muscularis was left intact, and the ring was positioned between two halves of a custom-made Ussing pressure chamber as described previously (31,32). The tissue was equilibrated for 45-60 min. Tissue preparations were used only if their TER was >1,000 $\Omega \cdot cm^2$. At different times, a square current pulse (10 μA for 10 ms) was passed through the tissue, and the resulting voltage response was recorded using the Scope program (AD Instruments).

To stretch the bladder tissue, the level of buffer in the mucosal hemichamber was raised to the top of the upper Luer fitting (see Fig. 1 in Ref. 32) and sealed over a total of 2 min.

To determine the apical membrane capacitance (where 1 μF ≈ 1 cm^2), we modeled the epithelium as an electrical circuit composed of an apical resistor and capacitor, a basolateral resistor and capacitor, and a series resistor. The equivalent equation for this circuit is as follows: $V(t) = I(t)[R_0 + R_1 (1 - e^{-t/R_1C_1}) + R_2(1 - e^{-t/R_2C_2})]$, where V is potential, I is current, R_1 and C_1 represent the apical umbrella cell resistance and capacitance, R_2 and C_2 represent the values for the basolateral plasma membrane (and possibly underlying cell layers), and R_0 is the series resistance. These data were transferred to PRISM software (GraphPad Software, San Diego, CA) and graphed, with time on the *x*-axis and the voltage response (at *time x*) on the *y*-axis. Data were graphed as means ± SE.

Cystometrograms

Mice were subjected to continuous-infusion cystometry with normal saline as described elsewhere (8). Experiments were done in accordance with an approved protocol from the University of Pittsburgh Institutional Animal Care and Use Committee (protocol no. 0309260). Flame-flanged PE-10 tubing connected to a pressure transducer and coupled to a computerized cystometrogram system (model DBA8000, World Precision Instruments) was inserted through the apical dome of the bladder. Tubing was implanted under urethane anesthesia and secured in place with a purse-string suture; voiding occurred naturally through the urethra. The mice were allowed to stabilize for 45-60 min as sterile saline was infused at 20 μl/min. After stabilization, the infusion rate was increased to 40 μl/min, and bladder activity was recorded. Throughout the cystometrogram procedures, animal temperatures were maintained with a water-heated pad and monitored by a rectal thermometer. At the end of the recording period, the mice were euthanized with inhalational CO_2.

RESULTS

Annexins in bladders of wild-type and knockout mice

Immunofluorescent staining of anxA4 in paraffin sections of relaxed, nondistended, whole bladders from control mice shows that the protein is present throughout all layers of the urothelium, including intermediate and basal cell layers, but is concentrated in the umbrella cells, which face the lumen (Fig. 1, *left*). No specific staining in situ was observed in anxA4a$^{-/-}$ animals. Because the other alternatively spliced anxA4 transcripts produce an identical protein, this result indicates that anxA4a is the only transcript expressed within the urothelium. Western blotting of control and knockout bladders reveals that annexins A1, A2, A3, A4, A5, and A6 are present in this tissue in wild-type animals but that anxA4 is selectively knocked out in this animal model (Fig. 1, *right*). There is no evidence at the level of immunoblotting for any compensatory increase in other annexins as a result of the loss of anxA4.

To obtain greater detail on the uroepithelial localization of various members of the annexin family and, specifically, to determine expression within subdomains of the urothelium, such as the umbrella cell layer and intermediate and basal layers, we used dissected bladders (no muscle) mounted in Ussing chambers on plastic rings with pins. The advantage of this approach is that it allows the application of a hydrostatic pressure to the urothelium and also “unfolds” the bladder for subsequent imaging. Bladders were fixed, cryosectioned, and then stained with polyclonal antibodies, as well as TO-PRO (for nuclei), as described in METHODS. Immunofluorescent staining of mounted bladders demonstrated that annexins A1, A2, A3, and A5 are present in the urothelium, while annexin A6 is less abundant (Fig. 2). Annexin 1 is found at highest concentrations within the umbrella cells and is present in the underlying epithelial layers as well. Annexin 2 appears strongly in umbrella cells and is present throughout the cytoplasm of the superficial cell layer. Annexin 3 appears to be concentrated

at the apical membrane of umbrella cells. Annexin 5 is also found at the apical membrane and, at lower levels, within all epithelial cell layers and exhibits intense staining in the underlying connective tissue. There is also clear evidence for annexin 5 association with the nuclear membrane (Fig. 2). The urothelium, therefore, exhibits a rich diversity of annexin isoforms, which presumably mediate a range of different cellular functions.

Stretch-induced redistribution of anxA4a in wild-type bladders

Since stretch and relaxation of the urothelium are important mechanical and physiological stimuli and since stretch has been shown to cause a rise in intracellular Ca^{2+} (30,32), we tested the hypothesis that stretch might induce some functional reorganization of anxA4a. Bladders from control mice were dissected to remove the muscle layer, mounted in Ussing chambers, and allowed to equilibrate in Krebs buffer at 37°C for 1 h; then a hydrostatic pressure was applied to the apical side of some bladders by addition of Krebs solution. We have found a substantial recovery of TER in tissue that is allowed to equilibrate after it is mounted in the chamber. TER of bladders stained in these experiments was 1,000-2,000 $\Omega \cdot cm^2$. A total pressure of 1 cmH_2O was added on the apical side and maintained for 1 h, then bladders (stretched and unstretched) were fixed in the chamber with paraformaldehyde. Confocal microscopy of bladders that were gently extended to remove folds and mounted on rings before staining shows a thin, three-cell-layer-deep urothelium that is anxA4 positive throughout all layers (Fig. 3*A*). Staining is specific for the epithelium. Confocal microscopy of bladders prepared in this way yields a more defined localization than immunohistochemistry of whole, nondistended bladders. Staining of anxA4a is fairly uniform across the umbrella, intermediate, and basal cells, with a predominantly diffuse cytoplasmic distribution. Interestingly, anxA4a is associated with the nuclei of umbrella cells (Fig. 3). This localization at the nuclear membrane is not evident within the intermediate and basal cells. Application of pressure/stretch to bladders results in striking changes to the distribution of anxA4a in the underlying epithelia (Fig. 3*B* and *inset*). It appears that anxA4a becomes concentrated at the cell borders. The relative size of the umbrella cells becomes apparent by inspection of the superficial epithelial cells. There are many basal cells for each umbrella cell nucleus. These data confirm that anxA4a within this specialized epithelium responds to a physiological stimulus, i.e., stretch, by translocating to cellular boundaries. This could be an important molecular response to bladder filling and voiding in vivo.

Uroepithelial barrier function

To explore the role of anxA4 within the urothelium, we used a mouse model in which the gene was ablated. By knocking out expression of the protein, it was hoped that certain physiological parameters of bladder function would be altered. We measured TER, water permeability, and urea permeability of excised bladders mounted in Ussing chambers. These parameters provide an indication of the barrier status of the bladder. The cohort of animals included 8 control and 9 $anxA4a^{-/-}$ males and 9 control and 12 $anxA4a^{-/-}$ females. There were no significant differences in the weights of gender-matched controls and knockout animals. As shown in Fig. 4, there was no statistically significant difference between any of these three parameters. TER was high (~3,000 $\Omega \cdot cm^2$), while water permeability ($3.23 \pm 0.3 \times 10^{-5}$ and $3.09 \pm 0.3 \times 10^{-5}$ cm/s for control and $anxA4a^{-/-}$, respectively) and urea permeability ($7.32 \pm 0.7 \times 10^{-6}$ and $8.2 \pm 0.9 \times 10^{-6}$ cm/s for control and $anxA4a^{-/-}$, respectively) are uniformly low, confirming that barrier function is intact in the $anxA4a^{-/-}$ animals and is equivalent to control animals.

Uroepithelial morphology

To investigate whether the loss of anxA4a had altered the epithelial ultrastructure, we studied bladders from control and $anxA4a^{-/-}$ animals under transmission and scanning

electron microscopy. Figure 5 shows a series of low- and high-magnification images of bladders from male and female mice. Low-power images show superficial umbrella cells, intermediate cells, and basal cells that comprise the transitional urothelium. Higher-power images show highly characteristic fusiform vesicles within umbrella cells. These subapical vesicles are thought to participate in stretch-activated exocytosis and insertion into the apical membrane (30), a response that permits the surface area of the bladder to increase during bladder filling with urine. There are no apparent macroscopic differences in cellular morphology between control and anxA4a$^{-/-}$ animals of either sex.

Scanning electron micrographs of bladders from male and female anxA4a$^{-/-}$ and control animals are shown in Fig. 6. Low-magnification images show the characteristic surface topology of the bladder. The luminal surface of umbrella cells is highly striated and folded (depending on the extent to which the bladder is filled or empty). The striations are attributable to the unique nature of the apical membrane in this organ, which is covered with a set of integral membrane proteins known collectively as the uroplakins. Uroplakins form a paracrystalline array within the apical membrane and cover up to 90% of the luminal surface area. Higher-magnification images show that the presence of this highly ordered protein array within the membrane results in a highly textured and scalloped membrane surface. The intersection of adjacent umbrella cells (e.g., 4 in Fig. 6*D*) can be seen by the presence of tight junctions (Fig. 6, *B*, *D*, *F*, and *H*). No changes in the uroepithelial ultrastructure were observed in the anxA4a$^{-/-}$ animals.

Stretch-activated trafficking

It has been shown that application of a hydrostatic pressure of a physiological magnitude to isolated and mounted rabbit bladders results in large increases in membrane capacitance, consistent with an increase in apical membrane surface area (30). Given the important role of annexins in membrane trafficking and membrane organization, impairment of, or alterations to, stretch-induced trafficking in the anxA4a$^{-/-}$ animals was investigated. The combined results of several experiments are shown in Fig. 7. As has been noted previously for rabbit bladder, application of pressure results in a biphasic response characterized by an initial rapid rate of increase in capacitance followed by a slower but consistent rate of increase over the next 4.5 h. In rabbits the increase is ~50%, whereas in mice capacitance increases by ~25%. This phenomenon has been shown to be reversible on release of pressure. Data for control and anxA4a$^{-/-}$ animals in Fig. 7*A* reveal that this function of the urothelium is unaffected by the absence of anxA4a. As shown in Fig. 7*B*, there are no changes in membrane capacitance in the absence of applied pressure.

Filling and voiding responses

To examine whether anxA4a$^{-/-}$ mice would show changes in gross bladder function, we performed cystometrograms on live animals. This technique, also known as continuous-infusion cystometry, measures intrabladder pressure and the timing of voiding cycles. These measurements allow an assessment of the overall functional status of the bladder, including the muscles and nerves that innervate the bladder, as well as the urothelium. The intravesical pressure traces in Fig. 8 show results for weight-matched (25- to 30-g body wt) controls and anxA4a$^{-/-}$ mice (n = 4 for controls and 2 for anxA4a$^{-/-}$). The frequency of voiding, intrabladder contraction pressure, and bladder capacities (~120 μl) were not qualitatively different between the two groups. Therefore, loss of anxA4a does not seem to affect bladder filling and emptying dynamics. It appears that the ability of the bladder to fill, expand, traffic membrane, send and receive sensory signals, and activate muscular contraction pressure is unaffected by the absence of uroepithelial anxA4a.

DISCUSSION

The role of annexins in different tissues and in different subcellular compartments remains an ongoing area of investigation. In the case of the urothelium, the role of these proteins is completely unknown. We show here for the first time that annexins A1, A2, A3, A4, A5, and A6 are found in the bladder and provide specific localization for several isoforms within the transitional epithelium. High levels of anxA4a are expressed in all three cell layers of the urothelium.

The highly conserved membrane binding motif and the functional response to elevated Ca^{2+} by annexins have led to efforts to define universal principles governing their cellular role. These efforts have not been completely successful, inasmuch as the variable NH_2 terminus confers distinct properties and distinct membrane-binding affinities on each annexin. A broad paradigm is that annexins are regulators of membrane function through effects on the lipids of the membrane itself, as well as through effects on integral membrane proteins, such as ion channels. Cumulatively, this leads to the view that annexins may be important modulators of Ca^{2+} homeostasis. Therefore, these proteins are not just regulated by Ca^{2+}; they actively function in return to control their own effector levels.

The widely expressed epithelial annexin anxA4 has been shown to be important in modulating apical membrane ion channel function. In T84 colonic epithelial cells, addition of purified anxA4 to the patch pipette inhibited Ca^{2+}-activated Cl^- channel activity, and, conversely, antibodies to anxA4 enhanced Cl^- currents (6,14). An indirect action of anxA4 is inhibition of the interaction of calmodulin-dependent kinase II with the Cl^- channel ClC3, perhaps by steric hindrance of phosphorylation site Ser^{109}. Also, anxA4 has also been shown to reduce membrane fluidity and permeability upon binding, suggesting that some of its functions may occur through direct physical effects on the lipid bilayer (11).

The bladder has long been viewed as a somewhat inert storage and collection vessel for urine. In recent years, however, persuasive evidence has accumulated to show that the urothelium and underlying musculature make up a highly innervated, dynamic, mechanosensitive system that responds to pressure and filling in a number of unique ways. These include activation of ion conductances, release of luminal and serosal ATP, activation of second messenger cascades, and dramatic upregulation of membrane-trafficking events, including coordinated exocytosis and endocytosis within the umbrella cell layer (3). Since the luminal surface of the bladder, i.e., the apical membrane of the urothelium, is one of the tightest and least permeable membranes in the body (7), we hypothesized that loss of anxA4a would lead to noticeable effects on overall bladder physiology. Several of the parameters we wished to measure operate through Ca^{2+} release pathways and so, we believed, might involve annexins. For example, hydrostatic pressure applied to rabbit bladders mounted in Ussing chambers causes increased exocytosis of fusiform vesicles in a Ca^{2+}-dependent manner (30,32). The presence of anxA4a within the bladder, in which anxA4a expression is limited to the urothelium (Figs. 1 and 3), suggests that stretch-induced increases of intracellular Ca^{2+} levels would certainly cause an increase in the membrane-binding activity of anxA4a. This prediction appears to be borne out in a selective manner by anxA4a association with the nuclear membrane in umbrella cells, a process not observed in the basal/intermediate cells. In those subluminal cell layers, however, there is an interesting redistribution of anxA4 to the cell periphery. It has been shown that anxA4 associates with the nuclear envelope in human fibroblasts (5,25) and in HEK 293 cells, which heterologously express the protein (24). In fibroblasts, anxA4 has a cytoplasmic and a nuclear localization. Elevations of intracellular and nuclear Ca^{2+} induced by A23187 result in a partial translocation of nuclear anxA4 to the nuclear membrane (5,25). This effect is dependent on a threshold concentration of Ca^{2+}. In the absence of extracellular Ca^{2+}, the

effect of A23187 on nuclear Ca^{2+} levels is reduced in duration and intensity. Under these conditions, anxA4 does not translocate (25). Interestingly, these fibroblasts were shown to also contain annexins 1, 2, 5, 6, and 7. Annexin 5 was the only other annexin found to bind the nuclear envelope in response to Ca^{2+}. In HEK 293 cells, elevated Ca^{2+} caused a translocation of cytoplasmic anxA4 to the nuclear envelope and the plasma membrane (24). The confocal images in this study suggest a similar relocation of anxA4a in bladder epithelium. In unstretched bladder, anxA4 is frequently present within the umbrella cell nucleus (Fig. 3*A*); in stretched bladder, however, the nucleus is sharply delineated by anxA4 at the nuclear membrane (Fig. 3*B*). This translocation may be initiated by stretch-induced increases in intracellular Ca^{2+}.

We conclude from this experiment that a physiological stimulus, such as tissue stretch, results in alterations to the distribution of anxA4a within the urothelium. It has been postulated that in cells with many different annexins, such as the urothelium, annexins in toto may form a sophisticated Ca^{2+} sensory system with a graded and interrelated response system (24). Each annexin has specific individual properties that create a unique functional identity that is dependent on a host of variables, including the intracellular environment; Ca^{2+} concentration, amplitude, and location; pH; and oxidation state. In addition, the target membrane or adjacent membrane chemistries are critical: the particular phospholipid composition, including the presence of cholesterol, ceramide, phosphatidylinositol phosphates, and transmembrane and peripheral membrane proteins and, finally, the annexin itself; its subunit association, self-association, binding, and docking proteins; phosphorylation status; and myristoylation. Although immunoblotting showed no compensatory increase in any of the other annexins in the anxA4a$^{-/-}$ animals, this does not preclude the possibility that functional redundancy could play a role in masking the loss of anxA4.

Despite the circumstantial evidence suggesting that anxA4a might be important in bladder physiology, we show that bladders from mice with no anxA4a exhibited normal barrier function as measured by TER (also implying that tight junction formation was not impaired in these animals), water permeability, and urea permeability. The bladders from these animals also exhibited normal morphology and cellular architecture and normal membrane-trafficking dynamics in response to stretch. These conclusions hold at the sensitivity level of the techniques used. Trafficking at the molecular/cellular level could be altered in ways that are not registered by capacitance readings. Voiding frequency and bladder contraction profiles were also indistinguishable between controls and anxA4a$^{-/-}$ animals. Therefore, the loss of anxA4a does not appear to affect any of the macroscopic properties that we have measured in these experiments. We speculate that anxA4a must play other, possibly more subtle, roles within the urothelium of the bladder. For instance, anxA4a may be responsible for the modulation of ion conductances in the bladder urothelium. It has been shown that the epithelial Na^{+} channel responsible for fine tuning Na^{+} balance in the collecting duct of the nephron is also present in the luminal membrane of the urothelium (28). This or other ion channels may be the molecular targets for regulation by anxA4a.

In the present study, we have identified stretch-dependent translocation of anxA4a in bladder epithelial cells from a uniform distribution throughout the cell to the nuclear and plasma membranes. Although these events are not necessary for normal bladder function, they may be required during other, as yet undefined, physiological challenges.

Acknowledgments

We thank Lay-Hong Ang (Beth Israel Deaconess Medical Center Confocal Imaging Core Facility) for valuable assistance, Elena Balestriere for capacitance measurements, and Giovanni Ruiz for scanning electron microscopy.

GRANTS

This work was supported by National Institute of Diabetes and Digestive and Kidney Diseases Grants DK-48217 (to M. L. Zeidel), R37-DK-54425 (to G. Apodaca), DK-41740 (to M. A. Kaetzel), and DK-46433 (to J. R. Dedman).

REFERENCES

1. Acharya P, Beckel J, Ruiz WG, Wang E, Rojas R, Birder L, Apodaca G. Distribution of the tight junction proteins ZO-1, occludin, and claudin-4, -8, and -12 in bladder epithelium. Am J Physiol Renal Physiol. 2004; 287:F305–F318. [PubMed: 15068973]
2. Almeida PF, Sohma H, Rasch KA, Wieser CM, Hinderliter A. Allosterism in membrane binding: a common motif of the annexins? Biochemistry. 2005; 44:10905–10913. [PubMed: 16086593]
3. Apodaca G. The uroepithelium: not just a passive barrier. Traffic. 2004; 5:117–128. [PubMed: 15086788]
4. Apodaca G, Kiss S, Ruiz W, Meyers S, Zeidel M, Birder L. Disruption of bladder epithelium barrier function after spinal cord injury. Am J Physiol Renal Physiol. 2003; 284:F966–F976. [PubMed: 12527557]
5. Barwise JL, Walker JH. Annexins II, IV, V and VI relocate in response to rises in intracellular calcium in human foreskin fibroblasts. J Cell Sci. 1996; 109:247–255. [PubMed: 8834809]
6. Chan HC, Kaetzel MA, Gotter AL, Dedman JR, Nelson DJ. Annexin IV inhibits calmodulin-dependent protein kinase II-activated chloride conductance. A novel mechanism for ion channel regulation. J Biol Chem. 1994; 269:32464–32468. [PubMed: 7798247]
7. Chang A, Hammond TG, Sun TT, Zeidel ML. Permeability properties of the mammalian bladder apical membrane. Am J Physiol Cell Physiol. 1994; 267:C1483–C1492.
8. Chopra B, Barrick SR, Meyers S, Beckel JM, Zeidel ML, Ford AP, de Groat WC, Birder LA. Expression and function of bradykinin B_1 and B_2 receptors in normal and inflamed rat urinary bladder urothelium. J Physiol. 2005; 562:859–871. [PubMed: 15576455]
9. Fiedler K, Lafont F, Parton RG, Simons K. Annexin XIIIb: a novel epithelial specific annexin is implicated in vesicular traffic to the apical plasma membrane. J Cell Biol. 1995; 128:1043–1053. [PubMed: 7896870]
10. Gerke V, Moss SE. Annexins: from structure to function. Physiol Rev. 2002; 82:331–371. [PubMed: 11917092]
11. Hill WG, Kaetzel MA, Kishore BK, Dedman JR, Zeidel ML. Annexin A4 reduces water and proton permeability of model membranes but does not alter aquaporin 2-mediated water transport in isolated endosomes. J Gen Physiol. 2003; 121:413–425. [PubMed: 12695484]
12. Hu P, Meyers S, Liang FX, Deng FM, Kachar B, Zeidel ML, Sun TT. Role of membrane proteins in permeability barrier function: uroplakin ablation elevates urothelial permeability. Am J Physiol Renal Physiol. 2002; 283:F1200–F1207. [PubMed: 12388410]
13. Junker M, Creutz CE. Ca^{2+}-dependent binding of endonexin (annexin IV) to membranes: analysis of the effects of membrane lipid composition and development of a predictive model for the binding interaction. Biochemistry. 1994; 33:8930–8940. [PubMed: 8043580]
14. Kaetzel MA, Chan HC, Dubinsky WP, Dedman JR, Nelson DJ. A role for annexin IV in epithelial cell function. Inhibition of calcium-activated chloride conductance. J Biol Chem. 1994; 269:5297–5302. [PubMed: 8106514]
15. Kaetzel MA, Hazarika P, Dedman JR. Differential tissue expression of three 35-kDa annexin calcium-dependent phospholipid-binding proteins. J Biol Chem. 1989; 264:14463–14470. [PubMed: 2527237]
16. Kennedy CR, Xiong H, Rahal S, Vanderluit J, Slack RS, Zhang Y, Guan Y, Breyer MD, Hebert RL. Urine concentrating defect in prosta-glandin EP_1-deficient mice. Am J Physiol Renal Physiol. 2007; 292:F868–F875. [PubMed: 16885154]
17. Lafont F, Lecat S, Verkade P, Simons K. Annexin XIIIb associates with lipid microdomains to function in apical delivery. J Cell Biol. 1998; 142:1413–1427. [PubMed: 9744874]

18. Lavelle J, Meyers S, Ramage R, Bastacky S, Doty D, Apodaca G, Zeidel ML. Bladder permeability barrier: recovery from selective injury of surface epithelial cells. Am J Physiol Renal Physiol. 2002; 283:F242–F253. [PubMed: 12110507]
19. Lavelle JP, Apodaca G, Meyers SA, Ruiz WG, Zeidel ML. Disruption of guinea pig urinary bladder permeability barrier in noninfectious cystitis. Am J Physiol Renal Physiol. 1998; 274:F205–F214.
20. Lecona E, Turnay J, Olmo N, Guzman-Aranguez A, Morgan RO, Fernandez MP, Lizarbe MA. Structural and functional characterization of recombinant mouse annexin A11: influence of calcium binding. Biochem J. 2003; 373:437–449. [PubMed: 12689336]
21. Li B, Dedman JR, Kaetzel MA. Intron disruption of the annexin IV gene reveals novel transcripts. J Biol Chem. 2003; 278:43276–43283. [PubMed: 12912993]
22. Liemann S, Huber R. Three-dimensional structure of annexins. Cell Mol Life Sci. 1997; 53:516–521. [PubMed: 9230929]
23. Luecke H, Chang BT, Mailliard WS, Schlaepfer DD, Haigler HT. Crystal structure of the annexin XII hexamer and implications for bilayer insertion. Nature. 1995; 378:512–515. [PubMed: 7477411]
24. Monastyrskaya K, Babiychuk EB, Hostettler A, Rescher U, Draeger A. Annexins as intracellular calcium sensors. Cell Calcium. 2007; 41:207–219. [PubMed: 16914198]
25. Raynal P, Kuijpers G, Rojas E, Pollard HB. A rise in nuclear calcium translocates annexins IV and V to the nuclear envelope. FEBS Lett. 1996; 392:263–268. [PubMed: 8774858]
26. Rescher U, Gerke V. Annexins— unique membrane binding proteins with diverse functions. J Cell Sci. 2004; 117:2631–2639. [PubMed: 15169834]
27. Rosengarth A, Gerke V, Luecke H. X-ray structure of full-length annexin 1 and implications for membrane aggregation. J Mol Biol. 2001; 306:489–498. [PubMed: 11178908]
28. Smith PR, Mackler SA, Weiser PC, Brooker DR, Ahn YJ, Harte BJ, McNulty KA, Kleyman TR. Expression and localization of epithelial sodium channel in mammalian urinary bladder. Am J Physiol Renal Physiol. 1998; 274:F91–F96.
29. Sohma H, Creutz CE, Gasa S, Ohkawa H, Akino T, Kuroki Y. Differential lipid specificities of the repeated domains of annexin IV. Biochim Biophys Acta. 2001; 1546:205–215. [PubMed: 11257523]
30. Truschel ST, Wang E, Ruiz WG, Leung SM, Rojas R, Lavelle J, Zeidel M, Stoffer D, Apodaca G. Stretch-regulated exocytosis/endocytosis in bladder umbrella cells. Mol Biol Cell. 2002; 13:830–846. [PubMed: 11907265]
31. Wang E, Truschel S, Apodaca G. Analysis of hydrostatic pressure-induced changes in umbrella cell surface area. Methods. 2003; 30:207–217. [PubMed: 12798135]
32. Wang EC, Lee JM, Ruiz WG, Balestreire EM, von Bodungen M, Barrick S, Cockayne DA, Birder LA, Apodaca G. ATP and purinergic receptor-dependent membrane traffic in bladder umbrella cells. J Clin Invest. 2005; 115:2412–2422. [PubMed: 16110327]

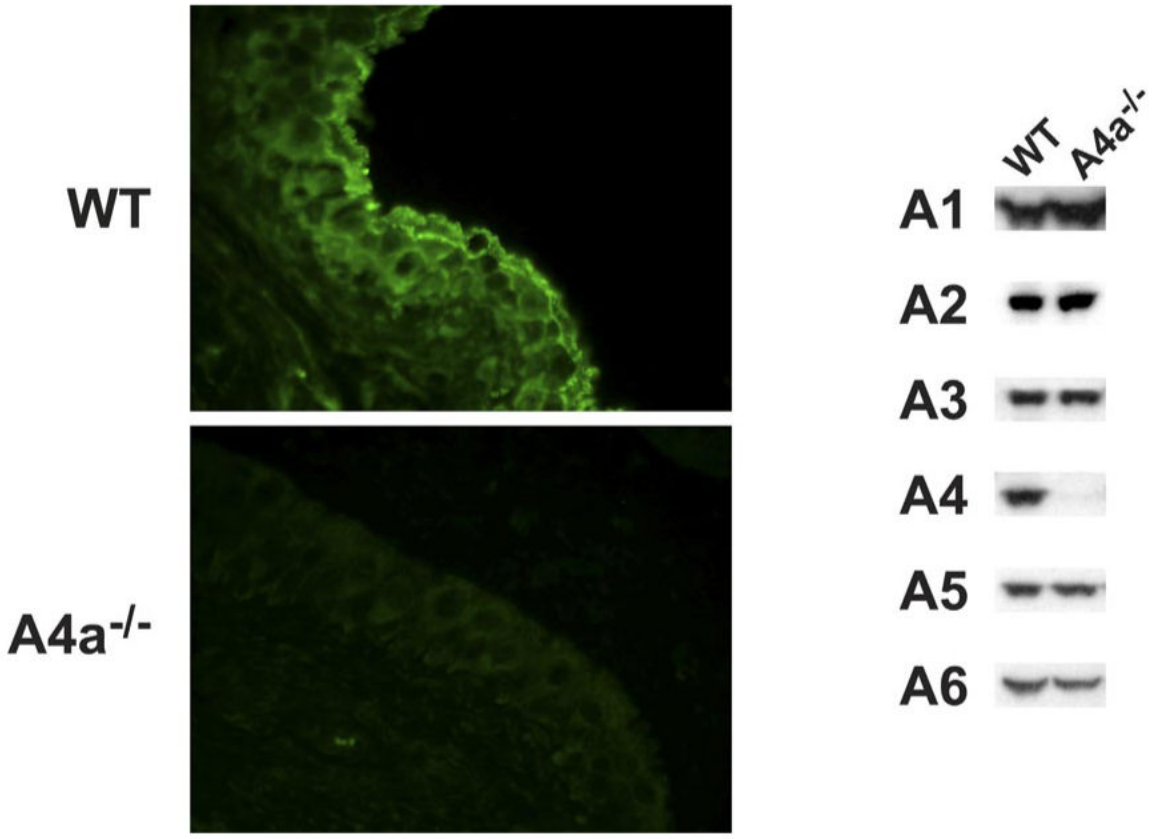

Fig. 1.

Left: annexin A4 immunolocalization in wild-type (WT) and annexin A4a-knockout (anxA4a$^{-/-}$) bladder. Annexin A4 is enriched in basal, intermediate, and umbrella cell layers of transitional epithelium. Magnification ×40, exposure time 0.25 s. *Right*: immunoblot analysis demonstrating presence of all 6 annexins in wild-type bladder. Annexin A4 is not expressed in bladders of A4a$^{-/-}$ mice, and there is no apparent compensatory overexpression of the other annexins.

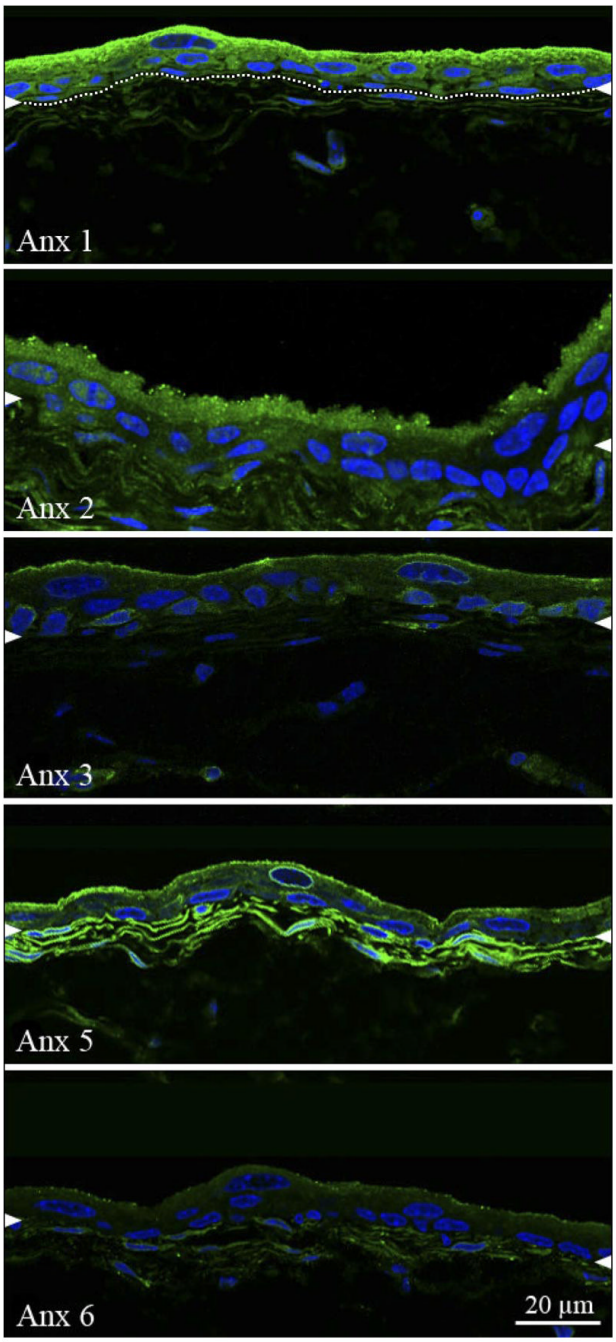

Fig. 2.

Immunofluorescent staining of different annexins within bladder epithelium. Distribution of annexins A1, A2, A3, A5, and A6 (Anx1 2, 3, 5, and 6) within the urothelium of muscle-stripped and Ussing chamber-mounted bladders was examined by confocal microscopy. Cryosectioned bladder sections were immunostained with each of the indicated antisera. Arrowheads indicate interface between epithelium and connective tissue. In annexin 1-stained image, dotted line shows this interface more clearly. Scale bar applies to all images.

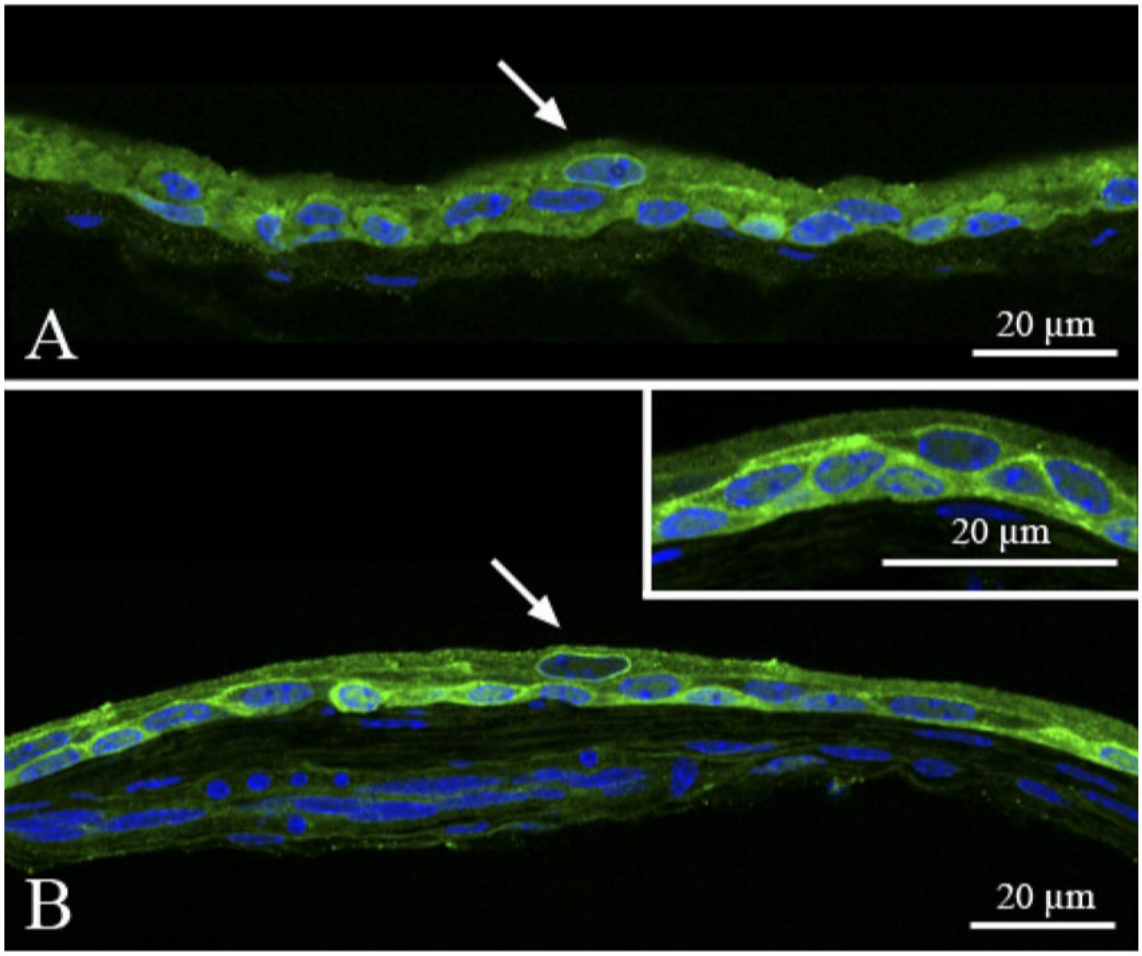

Fig. 3.

Annexin A4 immunofluorescence and confocal microscopy on unstretched (*A*) and stretched (*B*) bladders. Bladders were mounted in Ussing chambers, and then some were stretched by addition of buffer to the apical chamber (~1 cmH_2O). After 1 h, tissues were fixed in the chamber and then removed from the chamber and cryosectioned before they were immunostained for annexin 4 and confocal imaging. *Inset*: higher magnification of a different section of stretched bladder to emphasize staining pattern in underlying epithelial cells. Arrows denote umbrella cell nuclei.

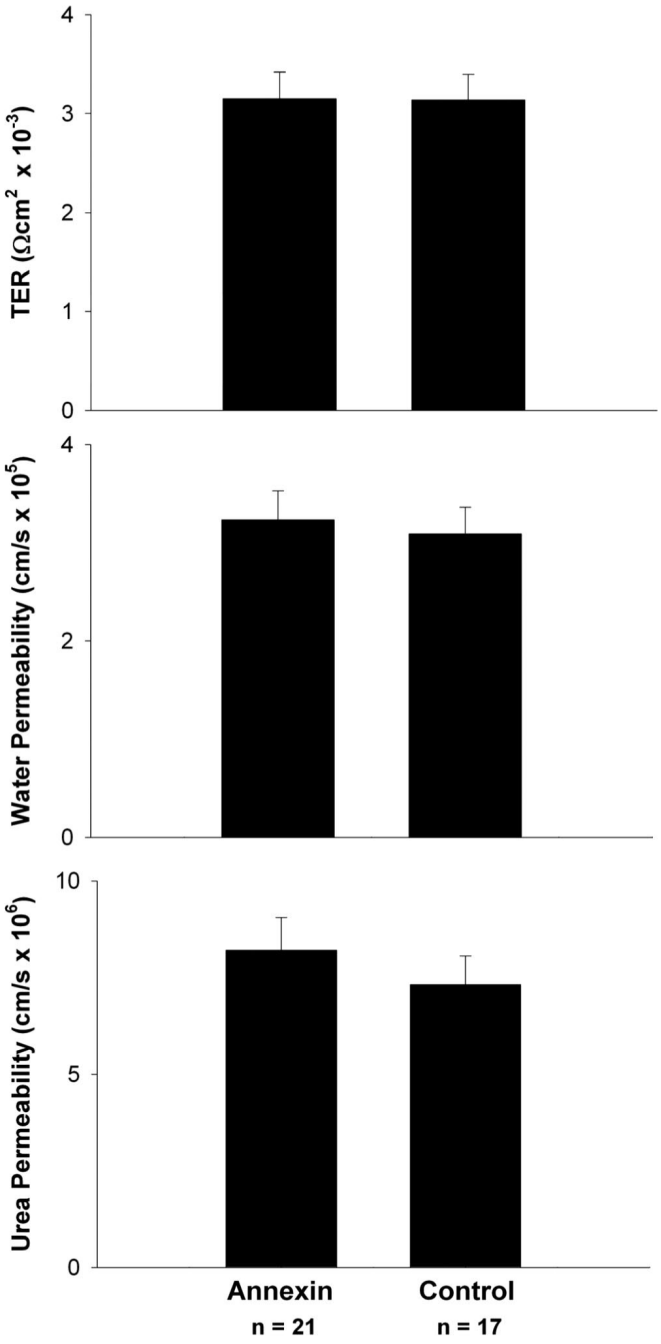

Fig. 4.

Transepithelial resistance (TER), apical membrane water permeability, and apical membrane urea permeability of bladders from male and female control and anxA4a$^{-/-}$ mice (Annexin). Values are means ± SE.

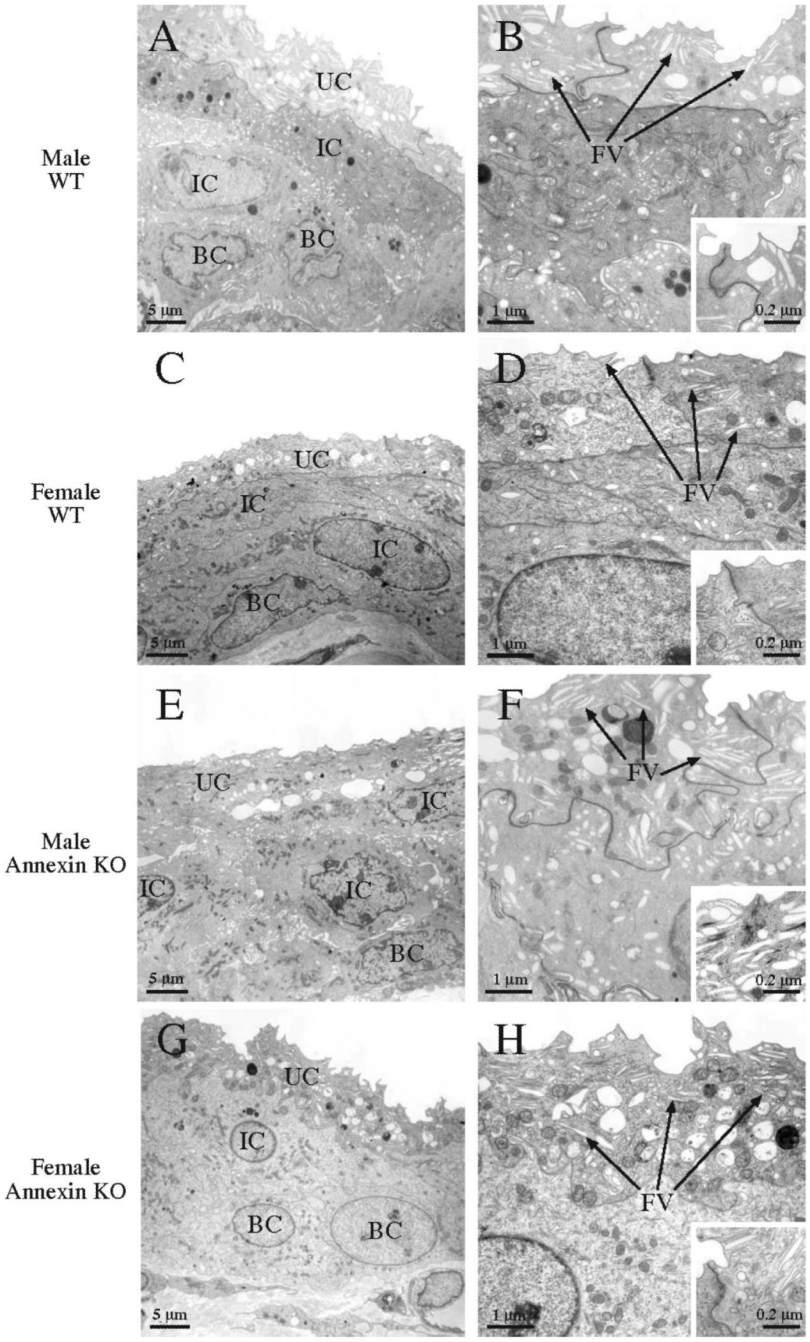

Fig. 5.

Transmission electron micrographs of male and female bladders from control (WT) and anxA4a$^{-/-}$ mice. Low-power images (*A*, *C*, *E*, and *G*) show umbrella cell layer (UC), intermediate cells (IC), and basal cells (BC). Higher-power images (*B*, *D*, *F*, and *H*) illustrate abundant presence of fusiform vesicles (FV) in umbrella cells and typical scalloped edges. *Insets*: tight junctions between adjacent cells.

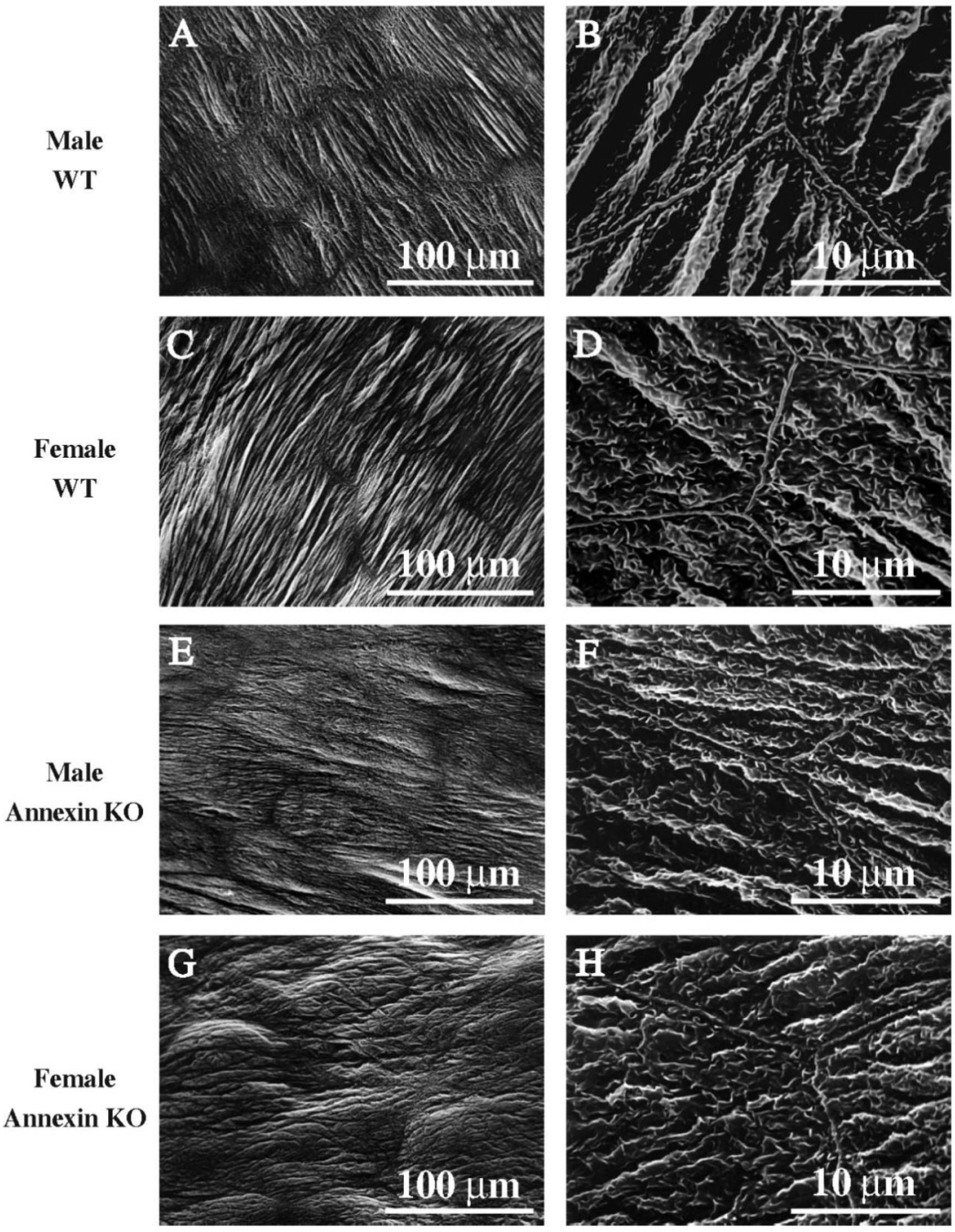

Fig. 6.

Scanning electron micrographs of male and female bladders from control (WT) and anxA4a$^{-/-}$ mice. Low-power images (*A*, *C*, *E*, and *G*) show surface morphology of bladders with typical striations and undulations. Higher-power images (*B*, *D*, *F*, and *H*) illustrate abundant presence of highly textured and scalloped apical membranes of individual umbrella cells. Tight junctions between adjacent cells can be seen in each of the images.

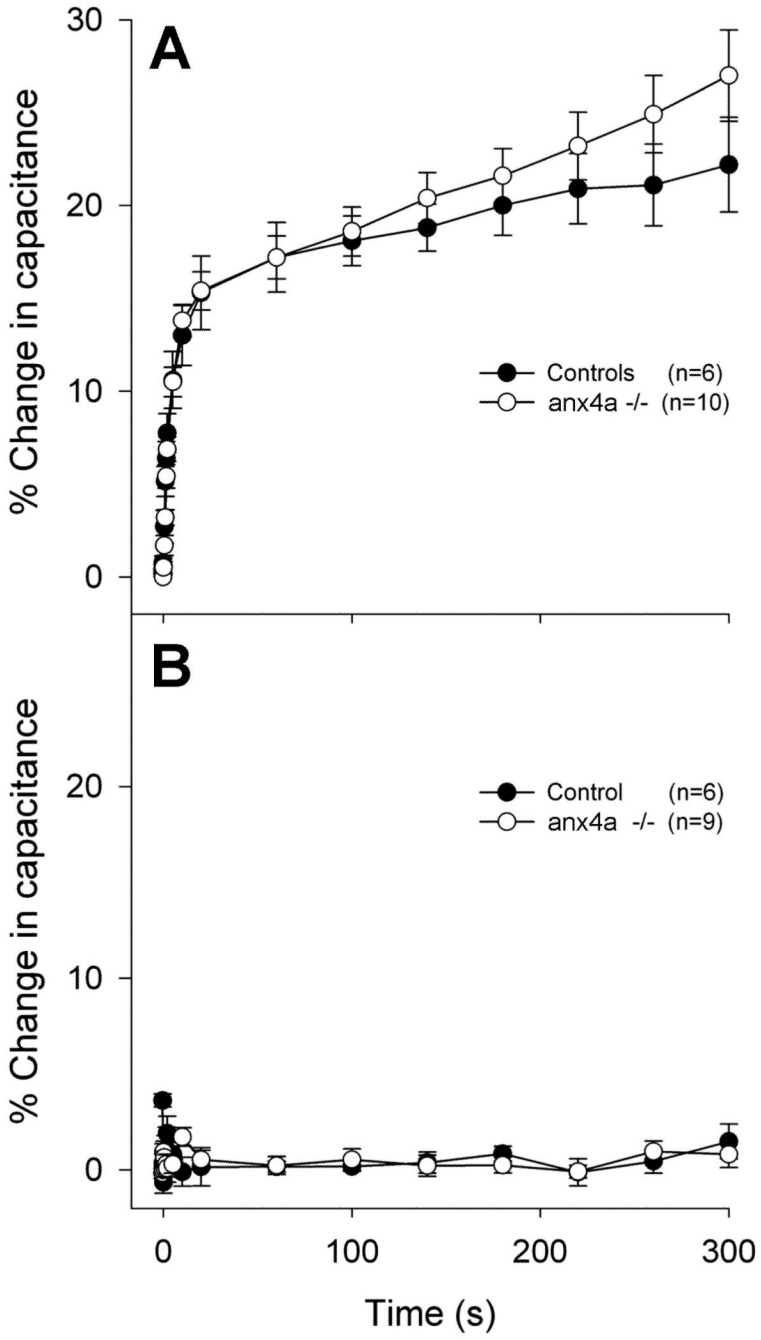

Fig. 7.

Change in capacitance over time in bladders from control and anxA4a$^{-/-}$ mice that were mounted in Ussing chambers and stretched by application of hydrostatic pressure (*A*) or left unstretched (*B*). Values are means ± SE.

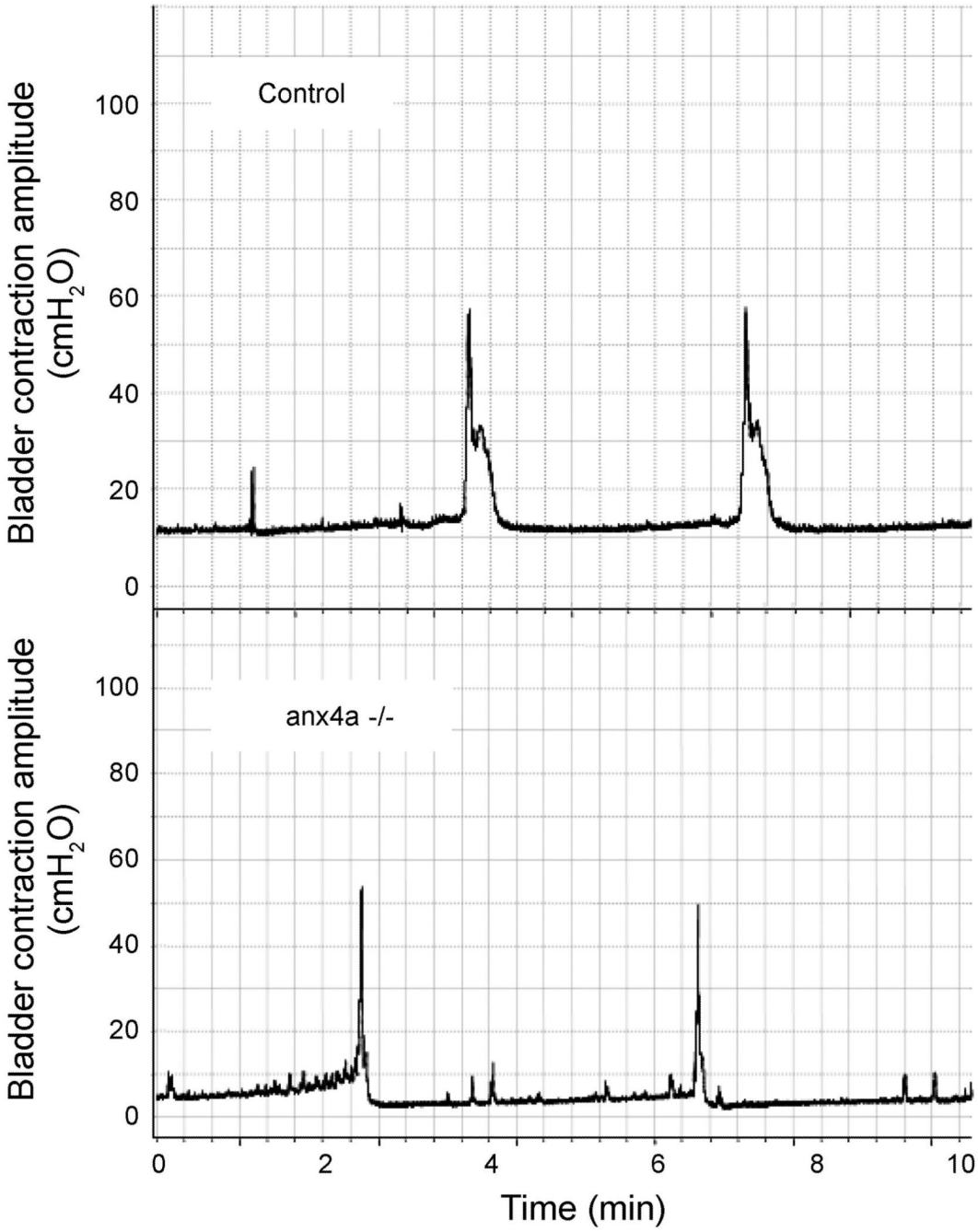

Fig. 8.

Cystometrograms of control and anxA4a$^{-/-}$ mice showing intravesical bladder pressure during filling and voiding cycles. Steep spikes correlate to muscle contraction and urine voiding. Contraction pressure, intervoid timing, and bladder volume data were obtained from bladders of mice that were continuously infused with saline (40 μl/min) for ≥1h.